Peak-to-average power ratio reduction for DCO-OFDM underwater optical wireless communication system based on an interleaving technique

Jurong Bai
Chenfei Cao
Yi Yang
Feng Zhao
Xiangjun Xin
Abdel-Hamid Soliman
Jiamin Gong

SPIE.

Peak-to-average power ratio reduction for DCO-OFDM underwater optical wireless communication system based on an interleaving technique

Jurong Bai,[a,*] Chenfei Cao,[a] Yi Yang,[a] Feng Zhao,[a] Xiangjun Xin,[a,b] Abdel-Hamid Soliman,[c] and Jiamin Gong[a]
[a]Xi'an University of Posts and Telecommunications, School of Electronic Engineering, Xi'an, China
[b]Beijing University of Posts and Telecommunications, School of Electronic Engineering, Beijing, China
[c]Staffordshire University, School of Engineering, Staffordshire, England, United Kingdom

Abstract. In underwater direct current-biased optical orthogonal frequency-division multiplexing (DCO-OFDM) system, high peak-to-average power ratio (PAPR) brings in-band distortion and out-of-band power. It also decreases the signal-to-quantization noise ratio of the analog-to-digital converter and the digital-to-analog converter. A time–frequency-domain interleaved subbanding scheme is proposed to reduce the PAPR of underwater DCO-OFDM system with low computation complexity and bit error rate (BER). The system BER is evaluated by the distances of the underwater optical wireless communication (UOWC), as well as by the signal attenuation of the UOWC channel. A least-square channel estimation method is adopted for adaptive power amplification at the receiver side, to further decrease the system BER. © *The Authors. Published by SPIE under a Creative Commons Attribution 3.0 Unported License. Distribution or reproduction of this work in whole or in part requires full attribution of the original publication, including its DOI.* [DOI: 10.1117/1.OE.57.8.086110]

1 Introduction

With growing interest in the research of ocean exploration, the requirement for high-speed, low link delay, and low implementation cost underwater communication technique has made underwater optical wireless communication (UOWC) an attractive alternative for radio-frequency (RF) and acoustic methods.[1] As an effective solution to intersymbol interference caused by the dispersive channel, orthogonal frequency-division multiplexing (OFDM) has been considered for both indoor and underwater optical communication systems to achieve high spectrum efficiency and data rate.[2,3] In optical OFDM (O-OFDM) systems, the adoption of intensity modulation with direct detection (IM/DD) requires the signal to be real and positive;[4] therefore, Hermitian symmetry transform and direct current (DC) bias addition are performed.[5] When the subcarriers of DC-biased O-OFDM (DCO-OFDM) signals happened to be in phase, high peak-to-average power ratio (PAPR) will bring serious signal distortion and performance deterioration, and result in nonlinear distortion when the signals passing through the power amplifier or laser diode (LD).[6]

There is few research concerning the PAPR reduction problem for the DCO-OFDM UOWC system. However, there has been research on OFDM PAPR reduction in a visible light communication (VLC) system. A pilot-assisted technique is proposed in Ref. 7, in which order statistics is utilized, and the frame with the least PAPR is selected. With an increase in the subcarriers, the computation complexity will grow, and the spectrum efficiency will decrease. An iterative clipping method in Ref. 8 reduces the PAPR of the VLC-OFDM system without out-of-band interference

(OBI), but the in-band distortion is inevitable, and the orthogonality of subcarriers may not be satisfied. Four kinds of VLC OFDM PAPR distributions are analyzed in Ref. 9, and the lower and upper clippings are taken into account. Tone reservation (TR) methods are adopted for VLC-OFDM to reduce PAPR in Refs. 10–12. The least squares approximation procedure is embedded into the signal-to-clipping noise ratio procedure in Ref. 10, which improves the convergence greatly. Time-domain kernel matrix (TKM) TR method is utilized in both Refs. 11 and 12. Different scaling vectors in the TKM-TR are generated by distinct sign vectors, and the one with the lowest PAPR is transmitted in Ref. 11. In Ref. 12, tailing is eliminated by optimizing the scaling factors, and the particle swarm optimization method is employed to obtain better clipping ratio (CR), but its PAPR reduction performance is limited. In Ref. 13, a simplified encoding structure real-valued interleaved single-carrier frequency-division multiplexing (I-SC-FDM) scheme is provided to reduce computation complexity, but its PAPR reduction performance is not good enough under 16QAM modulation.

In both VLC OFDM and UOWC systems, signal processing is basically the same. Their major difference lies in their channel models. In this paper, a time–frequency-domain-interleaved subbanding technique is proposed to reduce the autocorrelation of the input signal, which according to our theoretical analysis, will lead to further PAPR reduction. In the proposed method, time-domain and frequency-domain signals are interleaved together, which helps to decrease the autocorrelation of the input signal, and brings better PAPR reduction performance compared with the frequency-domain-interleaved method in Ref. 13. To evaluate the communication quality of the proposed method in UOWC system, the bit error rate (BER) performance is studied.

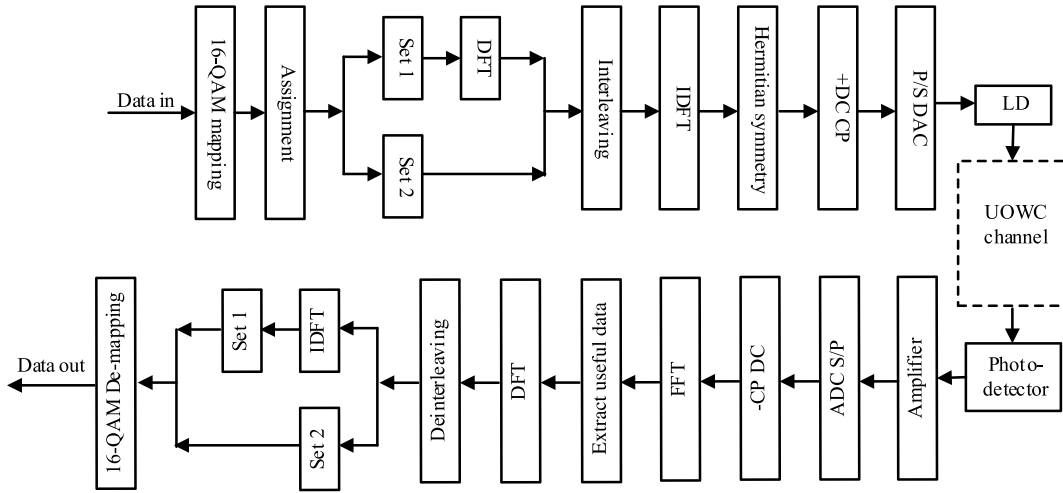*Address all correspondence to: Jurong Bai, E-mail: jurongbai@163.com

Fig. 1 Schematic diagram of UOWC system with the time–frequency-interleaved OFDM.

From UOWC channel model analysis and simulation results, it is shown that the underwater channel attenuates signals much more seriously as the communication distance grows, the system BER is mainly affected by the communication distance. In our proposed technique, a least-square (LS) channel estimation is employed at the receiver side, to adaptively adjust the power amplifier with the estimated underwater channel response, so as to effectively balance the channel attenuation and to obtain a better BER performance.

2 PAPR Reduction Based on Time–Frequency-Domain Interleaved OFDM

2.1 Time-Frequency-Domain-Interleaved Scheme

The proposed interleaved scheme for UOWC system is shown in Fig. 1. Through 16-QAM, the input binary bits $\mathbf{x}$ are modulated into frequency-domain $\mathbf{X} = [X_0, X_1, X_2, \ldots, X_{N-1}]$, where N is the number of subcarriers. In our proposed scheme, $\mathbf{X}$ is divided into two sets of signals. Set 1: $\mathbf{X}_1 = [X_0, X_1, X_2, \ldots, X_{N/2-1}]$, and set 2: $\mathbf{X}_2 = [X_{N/2}, X_{N/2+1}, X_{N/2+2}, \ldots, X_{N-1}]$. Set 1 is operated with discrete Fourier transform (DFT) to obtain $\mathbf{x}_1$, with its element expressed as

$$x_1(n) = \frac{1}{N/2-1} \sum_{k=0}^{N/2-1} X_1 e^{j\frac{2\pi nk}{N/2}}, \quad n = 0, 1, \ldots, N/2-1. \tag{1}$$

Set 2 does not go through DFT operation to reduce signal aperiodic autocorrelation, and to save computation complexity. Next, $\mathbf{x}_1$ and $\mathbf{X}_2$ are connected to produce $\mathbf{X}'_{1 \times N} = [\mathbf{x}_1 \quad \mathbf{X}_2]$.

As shown in Fig. 2, $\mathbf{X}'_{1 \times N}$ interleaves its time-domain part and frequency-domain part to produce $\hat{\mathbf{X}}$, whose inverse discrete Fourier transform (IDFT) is the time domain OFDM signal $\hat{\mathbf{x}}^t$. PAPR is defined as

$$\text{PAPR(dB)} = 10 \log \frac{\max_{0 \le n \le N-1}\{|\hat{x}^t|^2\}}{\text{E}\{|\hat{x}^t|^2\}}. \tag{2}$$

2.2 Theoretical Analysis on PAPR Reduction of Interleaved OFDM Signals

The aperiodic autocorrelation of $\hat{\mathbf{X}}$ is defined as

$$R_{\hat{\mathbf{X}}}(k) = \sum_{t=0}^{N-k-1} \hat{\mathbf{X}}_{t+k}\hat{\mathbf{X}}_t^* \qquad k = 0, \pm1, \pm2, \ldots, \pm N-1. \tag{3}$$

The time-domain OFDM signals are

$$\hat{\mathbf{x}}^t(n) = \frac{1}{N} \sum_{k=0}^{N-1} \hat{\mathbf{X}}_k e^{jkn\frac{2\pi}{N}} \qquad n = 0, 1, \ldots, N-1. \tag{4}$$

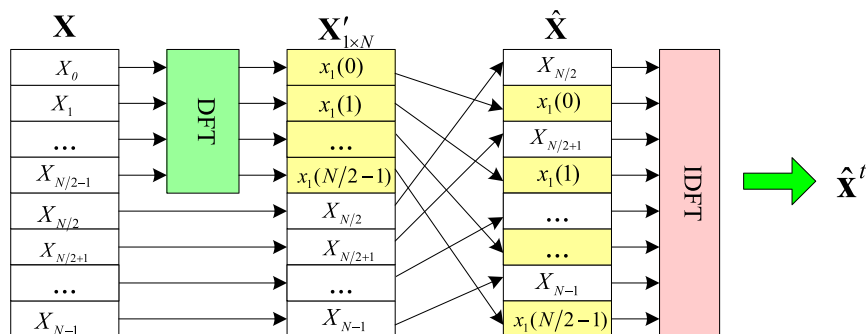The power of the time-domain OFDM signals can be expressed as

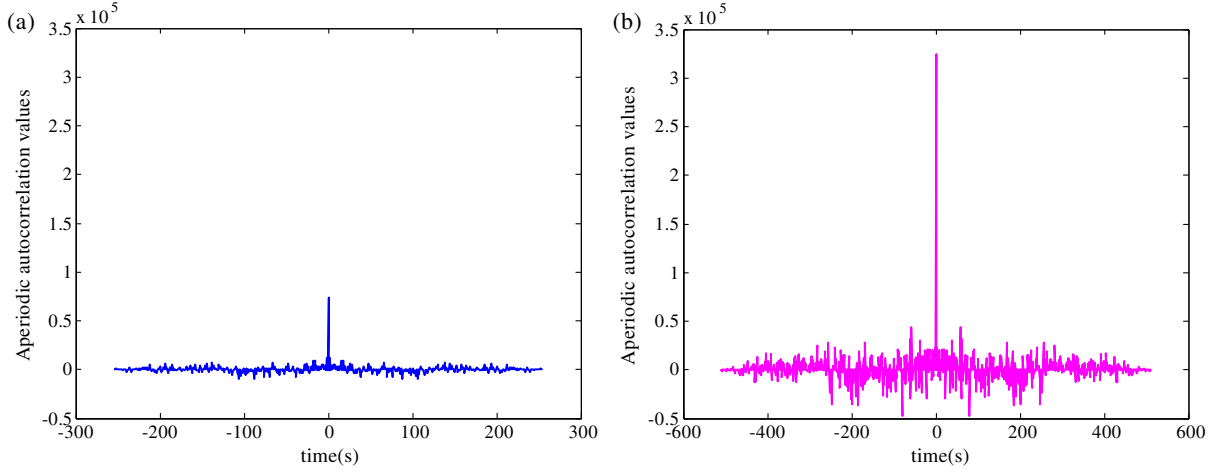**Fig. 2** The diagram of time–frequency-domain-interleaved scheme.

Fig. 3 Aperiodic autocorrelation value of different interleaved OFDM signals. (a) Proposed time–frequency-domain-interleaved OFDM scheme and (b) frequency–domain-interleaved scheme.[13]

$$|\hat{\mathbf{x}}^t(n)|^2 = \frac{1}{N^2} \sum_{t=0}^{N-1} \sum_{k=0}^{N-1} \hat{\mathbf{X}}_k \hat{\mathbf{X}}_t^* e^{j(k-t)n\frac{2\pi}{N}}$$

$$= \frac{1}{N^2} \left\{ \sum_{u=0}^{N-1} \hat{\mathbf{X}}_u \hat{\mathbf{X}}_u^* + 2\mathrm{Re}\left[\sum_{t=0}^{N-1} \sum_{k=t+1}^{N-1} \hat{\mathbf{X}}_k \hat{\mathbf{X}}_t^* e^{j(k-t)n\frac{2\pi}{N}} \right] \right\}$$

$$= \frac{1}{N^2} \left\{ \sum_{u=0}^{N-1} \hat{\mathbf{X}}_u \hat{\mathbf{X}}_u^* + 2\mathrm{Re}\left[\sum_{k=1}^{N-1} e^{jkn\frac{2\pi}{N}} \sum_{t=0}^{N-k-1} \hat{\mathbf{X}}_{t+k} \hat{\mathbf{X}}_t^* \right] \right\}$$

$$n = 0, 1, \ldots, N-1. \tag{5}$$

Substituting Eq. (3) into Eq. (5), the power of time-domain OFDM signals are updated as

$$|\hat{\mathbf{x}}^t(n)|^2 = \frac{1}{N^2} \left\{ R_{\hat{\mathbf{X}}}(0) + 2\mathrm{Re}\left[\sum_{k=1}^{N-1} e^{jkn\frac{2\pi}{N}} R_{\hat{\mathbf{X}}}(k) \right] \right\}$$

$$n = 0, 1, \ldots, N-1. \tag{6}$$

For any complex z, $\mathrm{Re}(z) \leq |z|$ and $\sum z_n \leq \sum |z_n|$. Therefore

$$\max\{|\hat{x}^t(n)|^2\} \leq \frac{1}{N^2} \left\{ R_{\hat{\mathbf{X}}}(0) + 2\sum_{k=1}^{N-1} |R_{\hat{\mathbf{X}}}(k)| \right\}$$

$$n = 0, 1, \ldots, N-1. \tag{7}$$

From Eq. (7), it can be concluded that the peak power of $\hat{\mathbf{x}}^t$ is proportional to the aperiodic autocorrelation of $\hat{\mathbf{X}}$. When the aperiodic autocorrelation of $\hat{\mathbf{X}}$ is small, the peak power value of the time-domain OFDM signal is small. We compare the proposed time–frequency-domain-interleaved scheme with the frequency-domain-interleaved scheme proposed in Ref. 13. Figure 3 shows the signal aperiodic autocorrelation value of the two schemes. It can be seen from Fig. 3(a) that its aperiodic autocorrelation value is obviously lower than 3(b). As the proposed scheme interleaves time-domain and frequency-domain signals together, its aperiodic autocorrelation value is thereby decreased effectively, which will leads to remarkable PAPR reduction.

3 System Model

3.1 DCO-OFDM UOWC System with PAPR Reduction

The IM/DD in O-OFDM systems require the signal to be both real and positive. To turn the PAPR reduced time-domain complex signal $\hat{\mathbf{x}}^t$ into a real one, Hermitian symmetry is operated, in which $\hat{\mathbf{x}}^t = [\hat{x}_0^t, \hat{x}_1^t, \ldots, \hat{x}_{N-1}^t]$ is expanded to produce $\hat{\mathbf{x}}^{t'} = [0, \hat{x}_0^t, \hat{x}_1^t, \ldots, \hat{x}_{N-2}^t, \hat{x}_{N-1}^t, 0, \hat{x}_{N-1}^{t*}, \hat{x}_{N-2}^{t*}, \ldots, \hat{x}_1^{t*}, \hat{x}_0^{t*}]$ for $2(N+1)$-point IFFT, and result in a real signal $\hat{\mathbf{x}}^{\hat{t}}$. Here, $(\cdot)^*$ denotes for complex conjugation operation. Next, DC-bias is added on $\hat{\mathbf{x}}^{\hat{t}}$ to ensure most negative signals become positive $\hat{\mathbf{x}}_p^{\hat{t}} = \hat{\mathbf{x}}^{\hat{t}} + B_{DC}$.[14] Here, the DC-bias $B_{DC} = U \cdot \sigma$, in which U is the DC-bias ratio, and $\sigma = \sqrt{\sum_{k=0}^{2N+1} [\hat{x}^{\hat{t}}(k) - \overline{x}]^2}$ is the standard deviation of $\hat{\mathbf{x}}^{\hat{t}}$.[15] However, there may still be some negative values in $\hat{\mathbf{x}}_p^{\hat{t}}$, therefore, clipping should be performed as

$$\hat{y}_p^t(n) = \begin{cases} \hat{x}_p^{\hat{t}}(n) & \hat{x}_p^{\hat{t}}(n) >= 0 \\ 0 & \hat{x}_p^{\hat{t}}(n) < 0 \end{cases},$$

$$n = 0, 1, \ldots, 2N+1. \tag{8}$$

After cyclic prefix (CP) addition and the parallel-to-series (P/S) conversion, the real and positive signals $\hat{\mathbf{y}}_p^t$ go through the digital-to-analog converter for LD underwater optical transmission. At the receiver side, the photodetector transmits the received signal to the amplifier. The remaining steps are basically the inverse operations of the transmitter as shown in Fig. 1.

3.2 UOWC Channel Model

According to the absorption and scattering in the underwater channel, the propagation loss factor for UOWC can be expressed as[16]

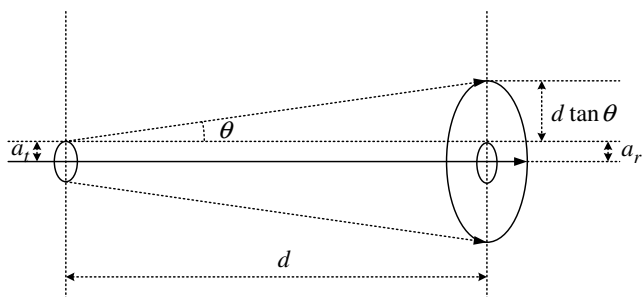$$L_P(\lambda, d) = e^{-c(\lambda)d}, \tag{9}$$

Fig. 4 Light spot expansion brought by light source divergence angle.

where λ is the operating wavelength, $c(\lambda)$ is the overall attenuation that combines absorption and scattering coefficients, and d is the UOWC distance.

Moreover, the light source divergence angle θ will also affect the attenuation of optical signals in underwater transmission. The value of θ will lead to light spot expansion, which brings changes in the system performance. Figure 4 shows the geometric expansion of the divergence angle of the light source. Meanwhile, considering the optical transmit antenna and the receive antenna, as well as the aperture radius of the transmitting equipment a_t, the aperture radius of the receiving equipment a_r, the relationship between the transmitted power P_t and the received power P_r, UOWC direct light of sight channel can be expressed as[17]

$$P_r = P_t \cdot \eta_t \cdot \eta_r \cdot [a_r^2/(d \cdot \tan\theta + a_t)^2] \cdot e^{-c(\lambda,chl,D)\cdot d}.$$
(10)

The overall attenuation c is different with the types of seawater. For clear ocean water, its value is 0.151 with

the wavelength of transmitted laser to be 514 nm.[1] η_t is the transmitting efficiency of the transmitting equipment, η_r is the receiving efficiency of the receiving equipment, chl is the chlorophyll concentration, and D is the concentration of nonpigmented suspended particles in sea water. In the following simulations, parameters are selected as is shown in Table 1.

3.3 Channel Estimation Based on LS for UOWC

The attenuation of sea water can be treated as a multiplicative noise, and the amplifier at the receiver side can be viewed as a channel balance procedure to reduce system BER. In the proposed scheme, an adaptive amplifier is designed based on the LS channel estimation method.[18]

Suppose a pilot signal $\mathbf{P}$ is inserted at the transmitter. $\mathbf{H}$ is the channel response. $\mathbf{Z}$ is the system noise. The received signal is $\mathbf{Y} = \mathbf{H} \cdot \mathbf{P} + \mathbf{Z}$. Let $\hat{\mathbf{H}}$ be the estimated channel response, therefore, $\mathbf{Y} = \hat{\mathbf{H}} \cdot \mathbf{P}$. The cost function is $J(\hat{\mathbf{H}}) = \|\mathbf{Y} - \mathbf{P} \cdot \hat{\mathbf{H}}\|^2$. To find the solution for $\hat{\mathbf{H}}$, make

$$\frac{\partial J(\hat{\mathbf{H}})}{\partial \hat{\mathbf{H}}} = -2(\mathbf{P}^H \mathbf{Y}) + 2(\mathbf{P}^H \mathbf{P}\hat{\mathbf{H}}) = 0,$$
(11)

which produces $\hat{\mathbf{H}} = \mathbf{P}^{-1}\mathbf{Y}$. According to Eq. (10), the attenuation factor $k = P_r/P_t = \eta_t \cdot \eta_r \cdot [a_r^2/(d \cdot \tan\theta + a_t)^2] \cdot e^{-c(\lambda,chl,D)\cdot d}$, which decreases with the growth of the communication distance d. With the value of k given by LS channel estimation, the receiver adaptively adjusts the amplifier to produce $\hat{y}_p^t{}' = \hat{y}_p^t \times k/E\{\hat{\mathbf{H}}\}$. The schematic diagram of the UOWC system with the LS channel estimation and adaptive amplifier is shown in Fig. 5.

Table 1 Values selected for UOWC channel parameters.

η_t	η_r	a_r (m)	θ (mrad)	a_t (m)	c	λ (nm)	chl (mg/m³)	D (mg/L)
0.91	0.91	0.003	0.33	0.003	0.151	514	5	1

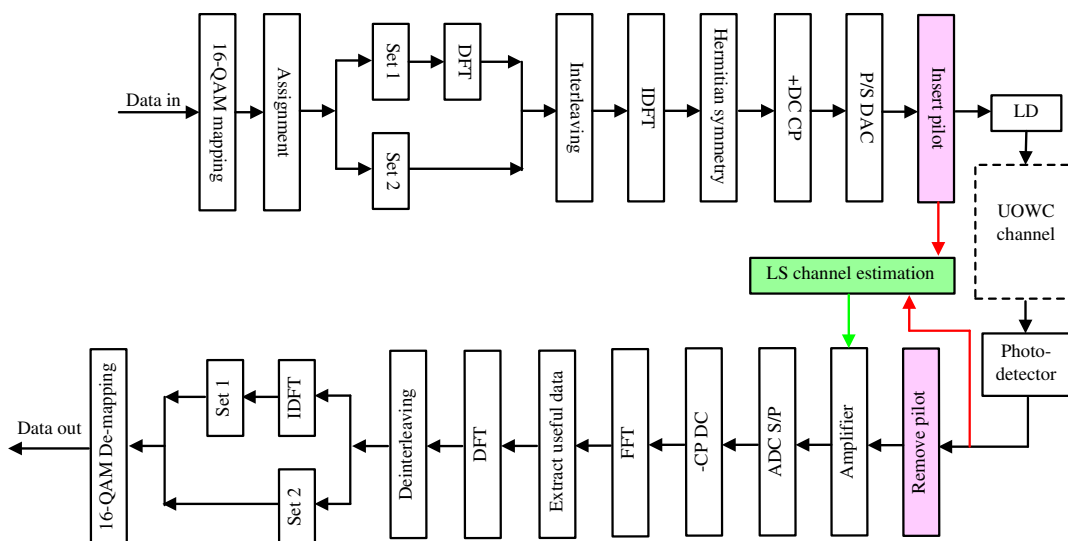**Fig. 5** Schematic diagram of UOWC system with LS channel estimation.
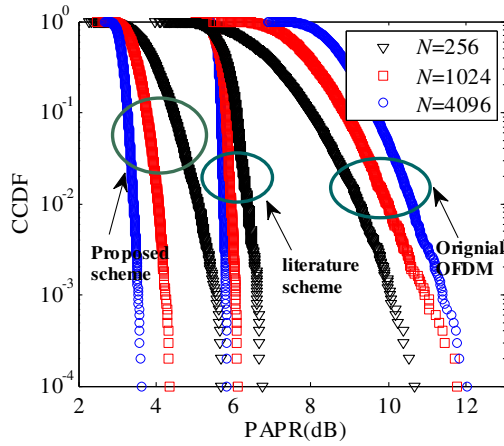
Fig. 6 CCDF statistics of OFDM symbols for different schemes.

Fig. 7 BER for different DC-biases.

Fig. 8 BER performance of 16-QAM DCO-OFDM UOWC system with $N = 1024$, $B_{DC} = 2$ in different amplifiers.

4 Simulation Results

The performances of the proposed time–frequency-domain-interleaved UOWC DCO-OFDM PAPR reduction scheme are evaluated through simulations. In the simulated DCO-OFDM UOWC system, the number of subcarriers is $N = 1024$, the oversampling factor is $J = 4$, and the length of the OFDM is CP = 32. The number of OFDM symbols is 1000, and 16-QAM is applied.

4.1 PAPR Reduction

The complementary cumulative distribution function (CCDF) is used to evaluate the PAPR reduction performance of the proposed scheme, which is shown in Fig. 6. The CCDF of PAPR is defined as: $\text{CCDF}(\text{PAPR}) = P\{\text{PAPR} > \text{PAPR}_o\}$, where PAPR_o is the PAPR destination value. It can be seen from Fig. 6 that in the proposed time–frequency-domain-interleaved scheme, the CCDF of PAPR can be remarkably reduced with an increase in the subcarriers. For the high-speed and high spectral efficiency optical interconnections, the subcarrier number is usually more than 1024, so as to obtain reasonably good performance.[19] When the subcarrier number is 1024 or 4096, the proposed time–frequency-domain-interleaved scheme can reduce the PAPR by 7.4 or 8.4 dB compared with the original OFDM signal, and can have 1.8 or 2.2 dB improvement compared with the frequency–domain-interleaved method proposed in Ref. 13.

4.2 Bit Error Rate Performance

The values of the DC-bias bring different performances of BER. The smaller the DC-bias is, the more serious the nonlinear distortion is, and the worse the BER is. With an increase in the DC-bias, the BER decreases. But high DC-bias reflects high optical power and low-power efficiency. Therefore, the selection of DC-bias should make a tradeoff between the optical power and the BER performance. Figure 7 shows the BER performances for different DC-bias values. When the DC-bias is >2, the BER is below 10^{-3}.

Figure 8 shows the BER performance for different UOWC distances and amplifier values. As discussed in Sec. 3.3, according to Eq. (10), the power attenuation factor $k = P_r/P_t$ is mainly affected by the UOWC distance d. The amplifier at the receiver side can partially counterbalance
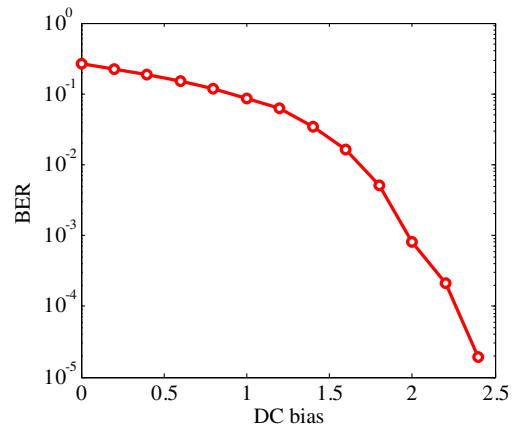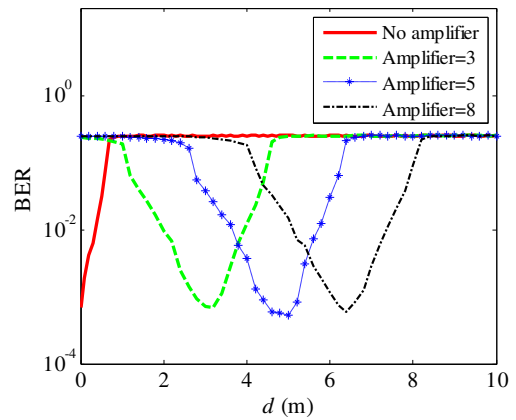
the attenuation of sea water; therefore, the value of amplifier can affect the system BER performance. The simulated curves show that when the amplifier = 3, the reliable communication distance is from 2.5 to 3.5 m, with its BER below 10^{-3}. When the amplifier = 5, the reliable communication distance is from 4.2 to 5.2 m. When the amplifier = 8, the reliable communication distance is from 5.8 to 6.8 m. It is found that for a certain value of amplifier, there is a best communication distance region to match with it. Similarly, for a certain region of UOWC distance, there is a value of amplifier to produce best BER performance. When the LS channel estimation method is adopted in the proposed time–frequency-domain-interleaved OFDM scheme, the system BER no longer deteriorates seriously with the UOWC distance, and its values keep near or below 10^{-3}. It has better BER performance compared with the scheme proposed in Ref. 13 and the clipping scheme, which is shown in Fig. 9.

4.3 Computational Complexity

In addition to the PAPR reduction performance and BER performance, the algorithm complexity is not negligible. Because of the additional DFT and IDFT operations, the computation complexity is mainly affected by the number of transmitter DFT and receiver IDFT. For an N-point DFT/IDFT, the number of complex multiplication and
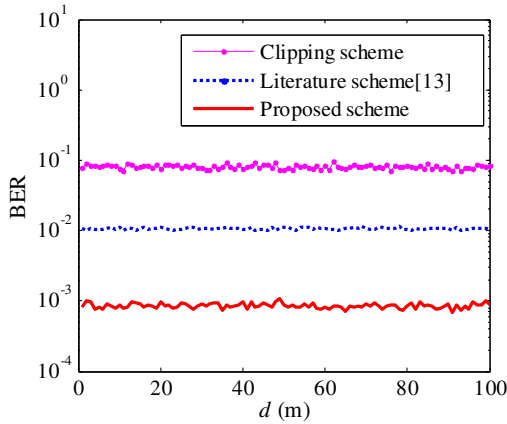
Fig. 9 BER performance of 16-QAM DCO-OFDM UOWC system with $N = 1024$, $B_{DC} = 2$ with adaptive amplifier for different distances.

Table 2 Computation complexity of different schemes.

	Complex multiplications	Complex additions
Conventional I-SC-FDM scheme	$2 \times N^2 = 2N^2$	$2N(N-1) = 2N^2 - 2N$
Proposed interleaved scheme	$2 \times \left(\frac{N}{2}\right)^2 = \frac{N^2}{2}$	$2 \times \left(\frac{N}{2}\right) \times \left(\frac{N}{2} - 1\right) = \frac{N^2}{2} - N$

complex addition is fixed. Table 2 compares the complexity for different schemes (the number of complex additions and complex multiplications).

5 Experimental Model

Figure 10 shows the experimental model for the UOWC VLC system. The PAPR reduced OFDM signals are generated offline with Matlab on a computer, and downloaded into the FPGA signal generator. The driver circuit and DC bias are designed to drive the LD for electrical to optical conversion. After reflections in the water tank by the mirrors at both ends, the optical signals are converted into electrical ones by an avalanche photodiode (APD). With the electrical amplifier (EA) and the decision regeneration circuit, the converted electrical signals are sent to the FPGA analyzer for the performance analysis.

Figure 11 shows the constellation of the received signals, in which $N = 1024$, $d = 10$ m, and amplifier = 20. It can be seen that the proposed time-frequency-domain-interleaved OFDM scheme has a clearer constellation compared with the I-SC-FDM scheme[13] and clipping scheme.

6 Conclusion

A time–frequency-domain-interleaved OFDM PAPR reduction scheme is proposed for the UOWC system. It can reduce the PAPR by 8.4 dB compared with the original OFDM signal. Compared with the traditional I-SC-FDM and clipping schemes, the performances of both PAPR and BER
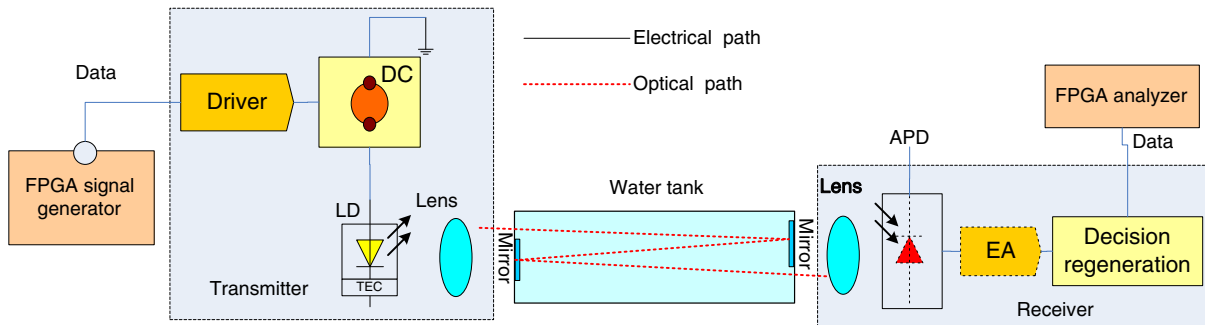

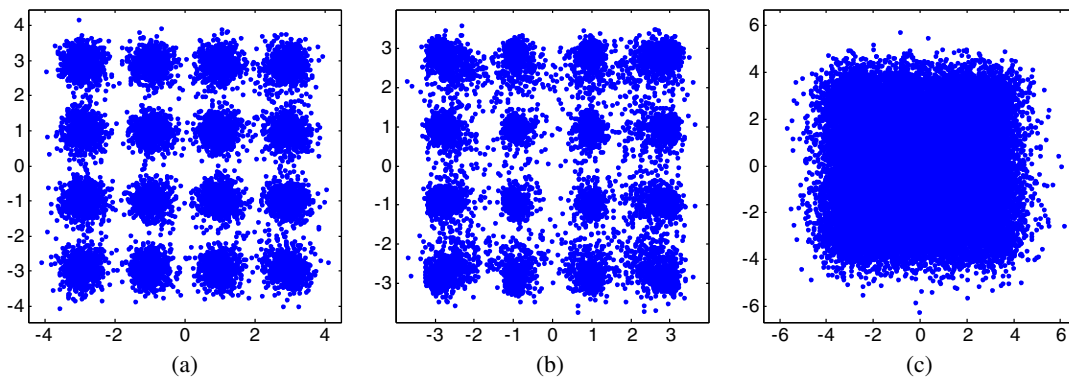**Fig. 10** Experimental model for UOWC VLC system.

Fig. 11 Constellation of the received signals. (a) Proposed time–frequency-domain-interleaved OFDM scheme, (b) frequency–domain-interleaved scheme,[13] and (c) clipping scheme.

are improved with low complexity cost. The system BER evaluation is mainly affected by the UOWC distance. The attenuation effect brought by the UOWC distance can be counterbalanced by the amplifier at the receiver side. An LS channel estimation method is adopted in the UOWC system to dynamically adjust the amplifier according to the estimated channel response. In this way, a better BER performance can be guaranteed for the UOWC system.

References

1. Z. Zeng et al., "A survey of underwater optical wireless communications," *IEEE Commun. Surv. Tutorials* **19**, 204–238 (2017).
2. J. Armstrong, "OFDM for optical communications," *J. Lightwave Technol.* **27**, 189–204 (2009).
3. W. Shieh and I. Djordjevic, *OFDM for Optical Communications*, Elsevier, Singapore (2011).
4. H. Chen et al., "Performance comparison of visible light communication systems based on ACO-OFDM, DCO-OFDM and ADO-OFDM," in *16th Int. Conf. on Optical Communications and Networks (ICOCN)*, pp. 1–3 (2017).
5. K. Nakamura, I. Mizukoshi, and M. Hanawa, "Optical wireless transmission of 405 nm, 1.45 Gbit/s optical IM/DD-OFDM signals through a 4.8 m underwater channel," *Opt. Express* **23**, 1558–1566 (2015).
6. H. Elgala, R. Mesleh, and H. Haas, "A study of LED nonlinearity effects on optical wireless transmission using OFDM," in *IFIP Int. Conf. on Wireless and Optical Communications Networks*, pp. 1–5 (2009).
7. F. B. Offiong, S. Sinanovic, and W. O. Popoola, "On PAPR reduction in pilot-assisted optical OFDM communication systems," *IEEE Access* **5**, 8916–8929 (2017).
8. Z. Yu, R. J. Baxley, and G. T. Zhou, "Iterative clipping for PAPR Reduction in visible light OFDM communications," in *33rd Annual IEEE Military Communications Conf.*, Baltimore, Maryland, pp. 1681–1686 (2014).
9. J. Wang et al., "PAPR analysis for OFDM visible light communication," *Opt. Express* **24**, 27457–27474 (2016).
10. J. Bai et al., "PAPR reduction based on tone reservation scheme for DCO-OFDM indoor visible light communications," *Opt. Express* **25**, 24630–24638 (2017).
11. P. Yu and S. Jin, "An enhanced TKM-TR method for PAPR reduction of OFDM signals with peak regrowth and peak residual reduced," in *8th IEEE Int. Conf. on Communication Software and Networks*, pp. 145–148 (2016).
12. Y. Hei et al., "Improved TKM-TR methods for PAPR reduction of DCO-OFDM visible light communications," *Opt. Express* **25**, 24448–24458 (2017).
13. J. Zhou et al., "Interleaved single-carrier frequency-division multiplexing for optical interconnects," *Opt. Express* **25**(9), 10586–10596 (2017).
14. M. M. A. Mohammed, C. He, and J. Armstrong, "Performance analysis of ACO-OFDM and DCO-OFDM using bit and power loading in frequency selective optical wireless channels," in *IEEE 85th Vehicular Technology Conf. (VTC Spring)*, pp. 1–5 (2017).
15. Y. Jiang et al., "Robust and low-complexity timing synchronization for DCO-OFDM LiFi systems," *IEEE J. Sel. Areas Commun.* **36**, 53–65 (2017).
16. H. Kaushal and G. Kaddoum, "Underwater optical wireless communication," *IEEE Access* **4**, 1518–1547 (2016).
17. F. Wang et al., "Characteristic analysis of underwater laser signal transmission channel based on visible light," *Opt. Commun. Technol.* **40**(3), 26–28 (2016), (in Chinese).
18. S. Coleri et al., "Channel estimation techniques based on pilot arrangement in OFDM systems," *IEEE Trans. Broadcast* **48**, 223–229 (2002).
19. F. Li et al., "High-level QAM OFDM system using DML for low-cost short reach optical communications," *IEEE Photonics Technol. Lett.* **26**(9), 941–944 (2014).

Jurong Bai is an associate professor at Xi'an University of Posts and Telecommunications. She received her BS and MS degrees in information and communication engineering from Xidian University, and is working toward her PhD in information and communication engineering from Northwestern Polytechnical University, China. Her current research interests include O-OFDM signal processing and wireless communication systems.

Chenfei Cao is a postgraduate student at Xi'an University of Posts and Telecommunications, China. He is working toward his MS degree in electronics and systems. His current research interests include optical signal processing and OFDM systems.

Yi Yang is an associate professor at Xi'an University of Posts and Telecommunications. She received her MS degree in information and communication engineering from Xi'an Jiaotong University. Her current research interests include optical signal processing, transmission, and optical communication systems.

Feng Zhao is a professor at the School of Electronic Engineering at Xi'an University of Posts and Telecommunications. His main research interests focus on information transmission and processing, signal measurement and control, and automatic detection devices.

Xiangjun Xin is a professor at the School of Electronic Engineering, and a member of the State Key Laboratory of Information Photonics and Optical Communications at Beijing University of Posts and Telecommunications. He received his PhD from Beijing University of Posts and Telecommunications in 2004. His main research interests focus on broadband optical transmission technologies, optical sensors, and all-optical networks.

Abdel-Hamid Soliman is an associate professor at Staffordshire University, UK. He is an honorary professor of Xi'an University of Posts and Telecommunications. He received his BEng degree (Hons) distinction with first-class honor in electronics and communications, his MSc degree in information systems and data acquisition systems, and his PhD in image processing. He is a member of IEEE and IET.

Jiamin Gong is a professor at the School of Electronic Engineering at Xi'an University of Posts and Telecommunications. He received his PhD in physical electronics and optoelectronics from Xi'an Jiaotong University in 1999. His main research interests focus on optical devices, materials, and all-optical networks.